Available online at www.sciencedirect.com
SCIENCE DIRECT®
Journal of Nuclear Materials 337–339 (2005) 305–309
journal of nuclear materials
www.elsevier.com/locate/jnucmat

Effect of $\mathbf{B}\times\nabla B$ direction on SOL energy transport in JET

W. Fundamenski [a,*], P. Andrew, K. Erents [a], A. Huber [b], G. Kirnev [c], G. Matthews [a], R. Pitts [d], V. Riccardo [a], S. Sipilä [e], EFDA JET contributors

[a] *Euratom/UKAEA Fusion Association, Culham Science Centre, Abingdon, OX 14 3DB, UK*
[b] *FZJ Julich GmbH/Euratom Institut für Plasmaphysik, TEC, Julich D-52425, Germany*
[c] *Moscow Nuclear Fusion Institute, RRC Kurchatov Institute, 123182 Moscow, Russia*
[d] *CRPP-EPFL, Association Euratom-Confédération Suisse, CH-1015 Lausanne, Switzerland*
[e] *Helsinki University of Technology, Euratom-Tekes Association, P.O. Box 2200, FIN-02015 HUT, Finland*

Abstract

The toroidal field and plasma current were reversed in recent JET experiments to yield a large number of good forward-reversed matched pairs. The direction, magnitude and scaling of the poloidal energy transport in the SOL can be explained by (neo-)classical drift-related heat fluxes ($\mathbf{E}\times\mathbf{B}$ and/or $\mathbf{B}\times\nabla T$) whose relative contribution scales as $\rho_{\theta s}/\lambda_{T_\sigma}$. Radial energy transport is largely independent of the $\mathbf{B}\times\nabla B$ direction, consistent with classical ion conduction.

PACS: 52.55.Fa; 52.65.Pp; 52.40.Hf; 52.25.Fi
Keywords: Cross-field transport; Edge plasma; Particle drifts; Plasma flow; Power deposition

1. Introduction

SOL energy transport occurs in three ($\|,\wedge,\perp$), rather than two ($\theta,\perp$), dimensions with respect to the local B-field. Since diamagnetic ($\wedge$) transport is largely due to classical drifts, it depends on the $\mathbf{B}\times\nabla B$ direction which we define as $\downarrow$ ($\uparrow$), fwd-B (rev-B) for short, as pointing towards (away from) the X-point. We thus expect SOL flows and divertor asymmetries to be sensitive to the $\mathbf{B}\times\nabla B$ direction, which is indeed observed. In contrast, it is not clear whether radial profiles, as measured by the integral power width λ_q which was found in dedicated fwd-B experiments [7–11] to scale as

$$\lambda_q^{\mathrm{all}} \propto A(Z)B_\phi^{-1}q_{95}^{0.6}P_t^{-0.4}n_{e,u}^{0.25} \quad (1)$$

would be affected by field reversal. Both (neo-)classical ion conduction [11] and ion orbit loss (IOL) can be reconciled with available fwd-B data (although the former gives a better fit). Since IOL is sensitive to $\mathbf{B}\times\nabla B$ [9,10], while classical conduction is not, field reversal can thus act as a method to distinguish between these theories.

2. Experiments

To test the above conclusions, dedicated rev-B experiments were recently performed on JET. High clearance magnetic configurations were used (described in detail in [9]), allowing the plasma to be slowly lifted as a rigid-body in order to characterise the deposited power

* Corresponding author. Tel.: +44 1235 464946; fax: +44 1235 464882.
E-mail address: wfund@jet.uk (W. Fundamenski).

0022-3115/$ - see front matter © 2004 Elsevier B.V. All rights reserved.
doi:10.1016/j.jnucmat.2004.08.030

profiles on the inner and outer divertors using Langmuir probes (LP) and embedded thermocouples (TC). Both B_ϕ and I_p were reversed, such that the magnetic helicity remained constant.

Four good discharges were obtained: one L-mode and three H-modes at different values of B_ϕ, I_p and P_{heat}. With the exception of the 2.5 MA/2.4 T H-mode, for which Type-I ELMs could not be obtained due to the higher III-I power threshold with rev-B [15], the discharges are fairly well matched in terms of power entering the SOL, $P_{SOL} = P_{heat} - P_{rad}$, i.e. heating minus core plasma radiative powers, and line average density $\langle n_e \rangle$; the majority (60–90%) of this power crosses the separatrix during the inter-ELM phase.

The total (ELM-averaged) deposited energy distribution on the divertor tiles was measured by TC analysis for the matched pairs of shots. The resulting out–in energy asymmetry is plotted versus P_{SOL} in Fig. 1; it is reduced from ~2.65 to 2.2 for fwd-B to ~1.7–1.9 for rev-B, with the average value roughly constant at 2.1 ± 0.05. The fractional energy asymmetry $\Delta E/\Sigma E \equiv (E_o - E_i)/(E_o + E_i)$ increases roughly linearly with P_{SOL} for H-mode plasmas, and is much larger for L-mode despite a lower power. This was also observed on a large sample (>100 shots) of unmatched fwd-B and rev-B shots from the same experimental campaign [12]. The L and H-mode asymmetries are comparable if the excess power above the L–H threshold, $P_{SOL} - P_{LH}$, is used for H-mode points, Fig. 1.

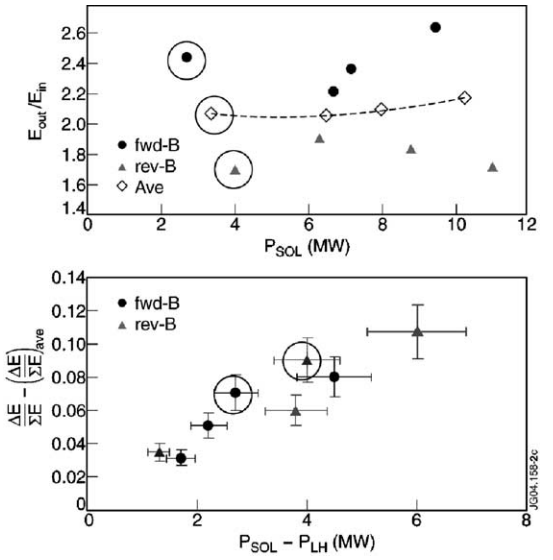

Fig. 1. Out–in energy asymmetry versus power into the SOL, and the $\Delta E/\Sigma E \equiv (E_o - E_i)/(E_o + E_i)$ versus power above L–H threshold. $(\cdot)_{ave}$ denotes an average of fwd-B and rev-B values. L-mode points are circled and P_{LH} is only subtracted from H-mode points.

In a recent review, the out–in power asymmetries under collisional (low P_{SOL}, high n_e) conditions were ascribed to an asymmetry in divertor radiation, with some evidence of drifts under less collisional conditions [1,2]. To test this hypothesis, the NBI heating power was increased from 2 to 8 MW in two matched fwd-B and rev-B JET L-modes (58850, 59557; 2.0 MA, 2.4 T). The target power was measured using transient analysis of the TC time traces, while careful radiation accounting was obtained using tomographic reconstructions of bolometric lines of sight. The results show a smaller divertor radiative fraction at higher input powers [13], so that target power asymmetries reflect actual changes of power flux into the divertor legs, $P_{div} = P_{target} + P_{rad,div}$. The change of P_{div} out–in asymmetry with $\mathbf{B} \times \nabla B$ direction ($P_{div,o}/P_{div,i} \sim 2.3$ for fwd-B versus ~1.3 for rev-B) suggests the SOL power flux has a strong component in the diamagnetic $\wedge$ (~poloidal) direction, for which classical $\mathbf{E} \times \mathbf{B}$ and diamagnetic drifts are obvious candidates [3–6]. This confirms the conclusions reached by Hutchinson et al. on the basis of reversed field experiments in Alcator C-mod [18].

The TC-measured peak heat flux q_{peak} values are plotted versus P_{SOL} in Fig. 2, together with LP measurements of peak electron heat flux. The out–in q_{peak} asymmetry (both TC and LP) ranges from 5 to 7 for $\mathbf{B} \times \nabla B\downarrow$, and 1.7–3.7 for $\mathbf{B} \times \nabla B\uparrow$. The ratio of total to electron power ($q_{tot}/q_e = q_{TC}/q_{LP}$, where $q_{LP} = 5T_e\Gamma_e$) in H-mode is smaller for fwd-B than for rev-B, 2–5 versus 1.2–1.8, respectively. Since the excess power is attributed to the ions ($q_i = q_{tot} - q_e$), this suggests that for fwd-B power entering the SOL is deposited is transferred mainly to the ions, while for rev-B it is more balanced between both species.

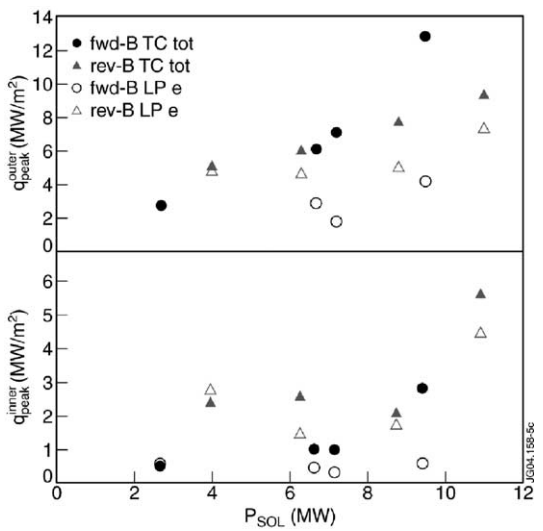

Fig. 2. Outer and inner, TC (total) and LP (electron) peak heat load values versus power into the SOL.

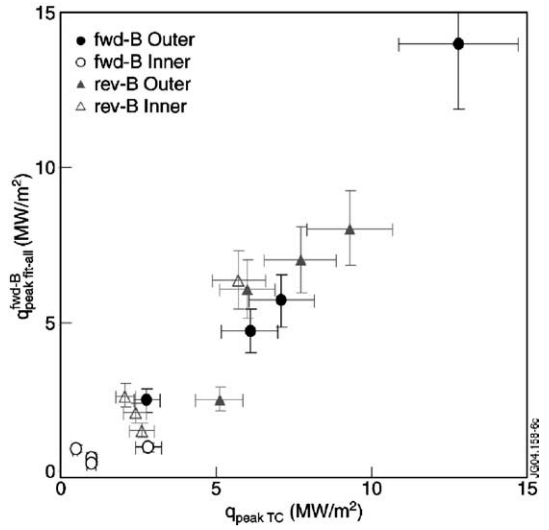

Fig. 3. TC measured (total) peak heat loads versus best fit to all outer, fwd-B, TC data, Eq. (1).

In order to assess the effect of field reversal, the above (TC) values were plotted versus the scaling $q_t \sim P_t/\lambda_q$ with λ_q, given by (1), derived from two dozen outer target fwd-B shots (mostly H-modes), Fig. 3. Within the measurement errors, the outer target rev-B H-mode points do not substantially differ from the fwd-B scaling, while the inner and L-modes points are only grossly correlated with the scaling. We conclude that under low collisionality (attached) conditions, the power width λ_q is insensitive to the $\mathbf{B}\times\nabla B$ direction. Since this quantity is directly related to the radial ($\perp$) heat diffusivity, $\lambda_q \sim (\chi_\perp \tau_\parallel)^{1/2}$, we may infer that radial energy transport in the SOL is largely *independent* of the $\mathbf{B}\times\nabla B$ direction, hence of classical drift effects – a most notable result!

3. Discussion

We are thus faced with three separate observations: (a) the average out–in power asymmetry of both P_{target} and P_{div} increases roughly linearly with P_{SOL}, (b) this asymmetry, for the same value P_{SOL}, is less sensitive to field reversal for the H-modes (ELM-averaged), than for L-modes, (c) radial ($\perp$) energy transport is largely independent of the $\mathbf{B}\times\nabla B$ direction. Roughly speaking, we find that the $\mathbf{B}\times\nabla B$ direction affects the poloidal (θ) but not the radial ($\perp$) energy transport. In this section we examine the implications of these results.

There is an overwhelming body of evidence [1,2] to suggest that the majority of the power enters the SOL on the low field side (LFS), near the outer mid-plane (omp); this is a consequence of (a) geometry (larger outboard area), (b) Shafranov shift compressing the flux surfaces on LFS, (c) bad curvature and the consequent increase in MHD-turbulence on LFS. These effects are independent of the $\mathbf{B}\times\nabla B$ direction, and with $R_o/R_i \sim L_{\parallel i}/L_{\parallel o} \sim 2$ predict an average out–in power asymmetry P_o/P_i of $\sim$2 (1.7 due to surface area alone) in agreement with Fig. 1.

In order to explain the $\mathbf{B}\times\nabla B$ dependence of P_o/P_i, we must consider the effects of drifts on energy transport in the SOL. Drift related energy fluxes can be obtained as [5,18–20]

$$\begin{aligned}\mathbf{q}_\sigma &\approx 2.5 p_\sigma \mathbf{v}_\sigma + 2.5 p_\sigma v_{t\sigma}\rho_\sigma \mathbf{b}\times\nabla T_\sigma/T_\sigma,\\ \mathbf{v}_\sigma &= v_{\parallel\sigma}\mathbf{b} + \mathbf{v}^E + \mathbf{b}\times(\nabla p_{\perp\sigma} - \mathbf{R})/m_\sigma n_\sigma \Omega_\sigma\\ &\quad + \{(v^2_{t\parallel\sigma} - v^2_{t\perp\sigma} + v^2_{\parallel\sigma})/\Omega_\sigma\}\mathbf{b}\times\mathbf{b}\cdot\nabla\mathbf{b},\end{aligned} \tag{2}$$

where $\mathbf{b} = \mathbf{B}/B$ is a unit vector, $\mathbf{v}^E \sim (1 + 0.25\rho_\sigma^2\nabla^2)\mathbf{E}\times\mathbf{b}/B \sim \mathbf{E}\times\mathbf{b}/B$ is the electrostatic drift velocity, $v_{t\parallel\sigma} = (T_{\parallel\sigma}/m_\sigma)^{1/2}$ and $v_{t\perp\sigma} = (T_{\perp\sigma}/m_\sigma)^{1/2}$ are thermal velocities, $\Omega_\sigma = e_\sigma B/m_\sigma$ is the gyro-frequency, $\rho_\sigma = v_{t\perp\sigma}/\Omega_\sigma \sim v_{t\sigma}/\Omega_\sigma$ the thermal gyro-radius, $\sigma \in \{i,e\}$ the species index, e_σ is the charge ($-$e for electrons, +Ze for ions). Dominant contributions to the θ (strictly speaking $\wedge$) components of (1) arise due to $\mathbf{E}\times\mathbf{B}$ and diamagnetic drifts. We write these explicitly as

$$\begin{aligned}&q^E_{\sigma\wedge} \sim 2.5 p_\sigma E_\perp/B_\phi, \quad q^{\nabla p}_{\sigma\wedge} \sim 2.5(T_\sigma/e_\sigma B_\phi)\nabla_\perp p_{\perp\sigma},\\ &q^{\nabla T}_{\sigma\wedge} \sim 2.5(p_\sigma/e_\sigma B_\phi)\nabla_\perp T_\sigma.\end{aligned} \tag{3}$$

Basic vector calculus suffices to show that diamagnetic heat fluxes are very nearly divergence free inside the plasma, $\nabla\cdot\mathbf{q}^{\nabla p}_\sigma \sim \nabla\cdot\mathbf{q}^{\nabla T}_\sigma \sim 0$. As such, they do not affect the energy dynamics of the plasma, which is determined by terms involving $\nabla\cdot\mathbf{q}_\sigma$, and can thus be neglected in most numerical simulations.

To first order, we can estimate the radial E-field as $E_\perp \sim 3\nabla_\perp T_{e,t}$ evaluated at the outer target. Writing the θ component of the $\parallel$ energy flux as $q_{\theta\sigma} = (B_\theta/B)q_{\parallel\sigma}$ with $q_{\parallel\sigma} \sim p_\sigma L_\parallel/\tau_{\parallel\sigma}$ and $\tau_{\parallel i} \sim L_\parallel/c_s$, $\tau_{\parallel e} \sim L^2_\parallel/\chi_{\parallel e}$, we find

$$\begin{aligned}&q^E_{i\theta}/q_{\theta i} \sim 3\nabla_\perp T_{e,t}/c_s B_\theta \sim 3\rho_{\theta s}/\lambda_{T_{e,t}}, \quad q^E_{e\theta}/q_{\theta e} \propto \nu^*_e \rho_{\theta s}/\lambda_{T_{e,t}},\\ &q^{\nabla T}_{i\theta}/q_{\theta i} \sim \nabla_\perp T_{\sigma,t}/c_s e_\sigma B_\theta \sim_\pm \rho_{\theta s}/\lambda_{T_i}, \quad q^{\nabla T}_{e\theta}/q_{\theta e} \propto \nu^*_e \rho_{\theta s}/\lambda_{T_e},\end{aligned} \tag{4}$$

where $c_s = \{(ZT_e + T_i)/m_i\}^{1/2}$ is the plasma sound speed. Hence the ratio of the poloidal components of the drift and parallel heat fluxes can be estimated as the gyro-radius normalised by the temperature gradient length, $\lambda_{T_\sigma} \equiv |\nabla_\perp T_\sigma/T_\sigma|^{-1}$. Since $\lambda_q \sim 3 - 5\rho_i \sim 1 - 1.5\rho_{\theta i}$ in high power H-modes on JET, with typical $\lambda_{T_\sigma} \sim 2 - 3\lambda_q$, we can expect $\rho_{\theta i}/\lambda_{T_i} \sim O(1)$ and thus a significant contribution from drift effects for low ν^*_i. Using the experimental $\lambda_q(1)$ as a rough guide for the λ_{T_σ} scaling, we find that the B-dependence cancels leaving a positive, roughly linear, power scaling,

$$\{q^E_{\sigma\wedge}, q^{\nabla T}_{\sigma\wedge}\}/q_{\wedge\sigma} \propto T^{0.5}_{\sigma,t} P^{0.5}_{SOL} n^{-0.2}_{e,u} \tag{5}$$

in agreement with experiment, Fig. 1 and [12,14]. This strongly suggests that the out–in divertor energy asymmetries are a direct consequence of classical ($\mathbf{E}\times\mathbf{B}$ and/or $\mathbf{B}\times\nabla T_i$) drift-related heat fluxes in the SOL.

To further quantify this conclusion, numerical simulations of matched fwd-B and rev-B discharges were performed using the EDGE2D transport code [16], with two sets of assumptions: (a) classical drifts, with the exception of divergence free (diamagnetic) terms; no radial pinch; (b) radial velocity (pinch) term with $v_\perp = 10$ m/s, directed towards the LFS for fwd-B and HFS for rev-B [14]. In each case, poloidally varying radial transport coefficients $\{D_\perp, \chi_\perp\}(\theta)$ were used, to simulate increased transport on the LFS. Both pure D and $D + C$ simulations were performed for each set of assumptions. The results are plotted versus $P_{\rm SOL}\mathbf{b}$ (negative values correspond to $\mathbf{B}\times\nabla B\downarrow$) in Fig. 4; also shown is the experimental data from Fig. 1, with $P_{\rm SOL}$ replaced by $P_{\rm SOL}/3$ for the L-mode points and $(P_{\rm SOL} - P_{\rm LH})/3$ for H-mode points, to compensate for the lower density used in the simulations, $n_{\rm eu}^{\rm EDGE2D}/n_{\rm eu}^{\rm JET} \sim 1/3$. The increase of P_o/P_i with input power is observed in all simulations, with the exception of the pinch velocity in a pure D plasma. Similar agreement is found with a larger L-mode data set [12,14]. This suggests a complicated coupling between mass and energy transport, in which classical drifts play a central role.

The role of direct ion orbit loss can now be properly assessed. This effect has been simulated using the guiding centre Monte-Carlo code ASCOT [17], in realistic JET magnetic geometry. The pedestal and SOL plasma profiles were taken for the fwd-B shot 50401 (2.5 MA/2.4 T, 12 MW NBI), which has previously been

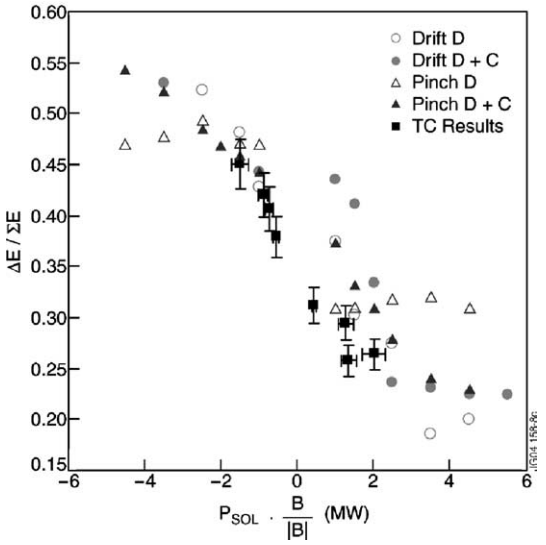

Fig. 4. Comparison of EDGE2D modelling to theory with $\Delta E/\Sigma E \equiv (E_o - E_i)/(E_o + E_i)$ versus power into the SOL.

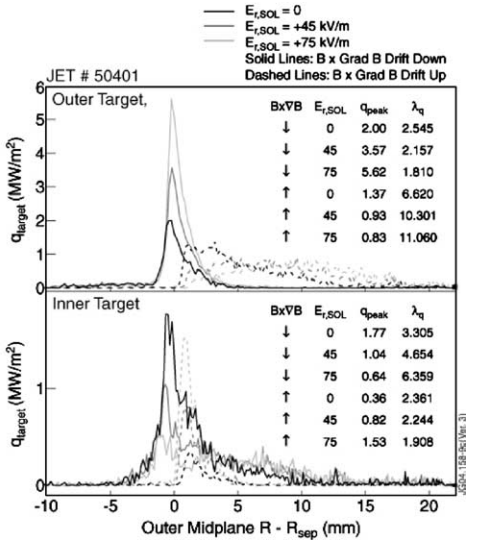

Fig. 5. ASCOT modelling of ion orbit loss target heat loads for 2.5 MA/2.4 T/12 MA JET shot (fwd-B versus rev-B); $E_{r,\rm SOL}$ (kV/m), λ_q (mm-omp).

modelled extensively and has the same field, current as the 50379/59691 pair, and similar heating power [9,10]. Self-consistent simulations were performed with a 15 mm-omp pedestal width, equivalent to $2.5\rho_{\theta i}$ at the outer mid-plane, with $T_{\rm i,ped} \sim 1.1$ keV and $T_{\rm i,sep} \sim 400$ eV. Three values of $E_{r,\rm SOL}$ were used: 0, 45 and 75 kV/m; only the largest field value yields ion peak powers >5 MW/m^2 as measured for this shot [9,10]. The results are shown in Fig. 5. The effect of field reversal on target power profiles is quite dramatic, with the outer profiles drastically broadened and peak values reduced, in contrast to experiment where little change in λ_q was observed, Fig. 3. We are thus forced to conclude that direct orbit loss is *not* responsible for the observed target profiles. More likely, IOL carries power down the pedestal gradient and into the SOL, where (neo-)classical conduction processes take over.

4. Conclusions

What have we learned from the new JET experiments? First, that field reversal affects the poloidal power flow into the divertor and hence power flow in the SOL; radiation asymmetries play a role only in highly collisional plasmas. Second, that the direction, magnitude and scaling of this poloidal power flow can be explained by classical drift-related heat fluxes ($\mathbf{E}\times\mathbf{B}$ and/or $\mathbf{B}\times\nabla T$) whose relative contribution can be estimated as $\rho_{\theta s}/\lambda_{T_\sigma}$; this conclusion is further backed up by numerical simulations using the EDGE2D code. Third, that radial transport is largely independent of

the $\mathbf{B}\times\nabla B$ direction; this key finding weighs heavily in favour of (neo-)classical ion conduction (no $\mathbf{B}\times\nabla B$ dependence) as the dominant SOL radial transport mechanism, and against the direct ion orbit loss (strong $\mathbf{B}\times\nabla B$ dependence). This is confirmed by detailed ASCOT simulations of IOL under realistic JET conditions. The only outstanding issue related to SOL energy transport are therefore issues related to ELMs, which will be the focus of future work.

References

[1] C.S. Pitcher, P.C. Stangeby, Plasma Phys. Control. Fus. 39 (1997) 779.
[2] P.C. Stangeby, The Plasma Boundary of Magnetic Fusion Devices, IoP, 2000.
[3] A. Chankin et al., Plasma Phys. Control. Fus. 36 (1994) 1853.
[4] A. Chankin et al., Plasma Phys. Control. Fus. 36 (1996) 563.
[5] A. Chankin, J. Nucl. Mater. 241–243 (1997) 199.
[6] A. Chankin, J. Nucl. Mater. 290–293 (2001) 518.
[7] V. Riccardo et al., Plasma Phys. Control. Fus. 43 (2001) 881.
[8] G.F. Matthews et al., J. Nucl. Mater. 290 (2001) 668.
[9] W. Fundamenski, Plasma Phys. Control. Fus. 44 (2002) 761.
[10] W. Fundamenski et al., J. Nucl. Mater. 313 (2003) 787.
[11] W. Fundamenski et al., Nucl. Fus. 44 (2004) 20.
[12] R. Pitts et al., these Proceedings, doi:10.1016/j.jnucmat.2004.10.111.
[13] A. Huber et al., these Proceedings, doi:10.1016/j.jnucmat.2004.10.123.
[14] G. Kirnev et al., these Proceedings, doi:10.1016/j.jnucmat.2004.09.032 and doi:10.1016/j.jnucmat.2004.10.143.
[15] Y. Andrew et al., Plasma Phys. Control. Fus. 46 (2004) 337.
[16] R. Simonini et al., Contrib. Plasma Phys. 34 (1994) 347.
[17] J.A. Heikkinen et al., Phys. Plasmas 8 (2001) 2824.
[18] I.H. Hutchinson et al., Plasma Phys. Control. Fus. 37 (1995) 1389.
[19] V.A. Rozhansky et al., Nucl. Fus. 41 (2001) 387.
[20] A.B. Mikhailovskii et al., Beit. Plasmaphys. 24 (1984) 335.